Tunable graphene antennas for selective enhancement of THz-emission

R. Filter,[1,*] M. Farhat,[1,2] M. Steglich,[3,4] R. Alaee,[1] C. Rockstuhl,[1] and F. Lederer[1]

[1]*Institute of Condensed Matter Theory and Solid State Optics, Abbe Center of Photonics, Friedrich-Schiller-Universität Jena, D-07743 Jena, Germany*
[2]*Division of Computer, Electrical, and Mathematical Sciences and Engineering, King Abdullah University of Science and Technology (KAUST), Thuwal, 23955-6900, Saudi Arabia*
[3]*Laboratory Astrophysics Group of the Max Planck Institute for Astronomy, Friedrich-Schiller-Universität Jena, D-07743 Jena, Germany*
[4]*Department of Chemistry, University of Basel, Klingelbergstrasse 80, CH-4056 Basel, Switzerland*
[*]*robert.filter@uni-jena.de*

Abstract: In this paper, we will introduce THz graphene antennas that strongly enhance the emission rate of quantum systems at specific frequencies. The tunability of these antennas can be used to selectively enhance individual spectral features. We will show as an example that any weak transition in the spectrum of coronene can become the dominant contribution. This selective and tunable enhancement establishes a new class of graphene-based THz devices, which will find applications in sensors, novel light sources, spectroscopy, and quantum communication devices.

OCIS codes: (020.4900) Oscillator strengths; (300.2140) Emission; (300.6390) Spectroscopy, molecular; (300.6495) Spectroscopy, terahertz.

References and links

1. P. Mühlschlegel, H.-J. Eisler, O. J. F. Martin, B. Hecht, and D. W. Pohl, "Resonant optical antennas," Science **308**, 1607–1609 (2005).
2. A. G. Curto, G. Volpe, T. H. Taminiau, M. P. Kreuzer, R. Quidant, and N. F. van Hulst, "Unidirectional emission of a quantum dot coupled to a nanoantenna," Science **329**, 930 (2010).
3. P. Anger, P. Bharadwaj, and L. Novotny, "Enhancement and quenching of single-molecule fluorescence," Phys. Rev. Lett. **96**, 113002 (2006).
4. B. S. Song, S. Noda, T. Asano, and Y. Akahane, "Ultra-high-q photonic double-heterostructure nanocavity," Nat. Mat. **4**, 207–210 (2005).
5. A. J. Campillo, J. D. Eversole, and H.-B. Lin, "Cavity quantum electrodynamic enhancement of stimulated emission in microdroplets," Phys. Rev. Lett. **67**, 437–440 (1991).
6. J.-J. Greffet, M. Laroche, and F. Marquier, "Impedance of a nanoantenna and a single quantum emitter," Phys. Rev. Lett. **105**, 117701 (2010).
7. F. H. L. Koppens, D. E. Chang, and F. J. Garcia de Abajo, "Graphene plasmonics: a platform for strong light-matter interactions," Nano Lett. **11**, 3370–3377 (2011).
8. R. Filter, S. Mühlig, T. Eichelkraut, C. Rockstuhl, and F. Lederer, "Controlling the dynamics of quantum mechanical systems sustaining dipole-forbidden transitions via optical nanoantennas," Phys. Rev. B **86**, 035404 (2012).
9. S. Karaveli and R. Zia, "Spectral tuning by selective enhancement of electric and magnetic dipole emission," Phys. Rev. Lett. **106**, 193004 (2011).
10. M. Tamagnone, J. Gomez-Diaz, J. Mosig, and J. Perruisseau-Carrier, "Analysis and design of terahertz antennas based on plasmonic resonant graphene sheets," J. Appl. Phys. **112**, 114915–114915 (2012).
11. M. Tamagnone, J. S. Gomez-Diaz, J. R. Mosig, and J. Perruisseau-Carrier, "Reconfigurable terahertz plasmonic antenna concept using a graphene stack," Appl. Phys. Lett. **101**, 214102 (2012).

#180026 - $15.00 USD Received 16 Nov 2012; revised 21 Jan 2013; accepted 23 Jan 2013; published 6 Feb 2013

12. R. Alaee, C. Menzel, C. Rockstuhl, and F. Lederer, "Perfect absorbers on curved surfaces and their potential applications," Opt. Express **20**, 18370–18376 (2012).
13. H. Boehm, A. Clauss, U. Hofmann, and G. Fischer, "Dünnste kohlenstoff-folien," Z. Naturforsch. B **17**, 150–153 (1962).
14. K. S. Novoselov, A. K. Geim, S. V. Morozov, D. Jiang, Y. Zhang, S. V. Dubonos, I. V. Grigorieva, and A. A. Firsov, "Electric field effect in atomically thin carbon films," Science **306**, 666–669 (2004).
15. A. H. Castro Neto, F. Guinea, N. M. R. Peres, K. S. Novoselov, and A. K. Geim, "The electronic properties of graphene," Rev. Mod. Phys. **81**, 109–162 (2009).
16. Z. Fei, G. O. Andreev, W. Bao, L. M. Zhang, A. McLeod, C. Wang, M. K. Stewart, Z. Zhao, G. Dominguez, M. Thiemens, M. M. Fogler, M. J. Tauber, A. H. Castro-Neto, C. N. Lau, F. Keilmann, and D. N. Basov, "Infrared nanoscopy of dirac plasmons at the graphene–sio2 interface," Nano Lett. **11**, 4701–4705 (2011).
17. J. Chen, M. Badioli, P. Alonso-González, S. Thongrattanasiri, F. Huth, J. Osmond, M. Spasenović, A. Centeno, A. Pesquera, P. Godignon, A. Z. Elorza, N. Camara, F. J. García de Abajo, R. Hillenbrand, and F. H. Koppens, "Optical nano-imaging of gate-tunable graphene plasmons," Nature (2012).
18. G. W. Hanson, "Dyadic greens functions and guided surface waves for a surface conductivity model of graphene," J. Appl. Phys. **103**, 064302 (2008).
19. S. Hasan, R. Filter, A. Ahmed, R. Vogelgesang, R. Gordon, C. Rockstuhl, and F. Lederer, "Relating localized nanoparticle resonances to an associated antenna problem," Phys. Rev. B **84**, 195405 (2011).
20. Y.-J. Yu, Y. Zhao, S. Ryu, L. E. Brus, K. S. Kim, and P. Kim, "Tuning the graphene work function by electric field effect," Nano Lett. **9**, 3430–3434 (2009).
21. L. Ju, B. Geng, J. Horng, C. Girit, M. Martin, Z. Hao, H. Bechtel, X. Liang, A. Zettl, Y. Shen, and F. Wang, "Graphene plasmonics for tunable terahertz metamaterials," Nat. Nanot. **6**, 630–634 (2011).
22. H. Yan, X. Li, B. Chandra, G. Tulevski, Y. Wu, M. Freitag, W. Zhu, P. Avouris, and F. Xia, "Tunable infrared plasmonic devices using graphene/insulator stacks," Nat. Nanotechnol. **7**, 330–334 (2012).
23. M. Jablan, H. Buljan, and M. Soljačić, "Plasmonics in graphene at infrared frequencies," Phys. Rev. B **80**, 245435 (2009).
24. W. Schumacher, M. Kühnert, P. Rösch, and J. Popp, "Identification and classification of organic and inorganic components of particulate matter via raman spectroscopy and chemometric approaches," J. Raman Spectrosc. **42**, 383–392 (2011).
25. W. Xu, X. Ling, J. Xiao, M. Dresselhaus, J. Kong, H. Xu, Z. Liu, and J. Zhang, "Surface enhanced raman spectroscopy on a flat graphene surface," PNAS **109**, 9281–9286 (2012).
26. W. Vogel and D. G. Welsch, *Quantum Optics* (Wiley, 2006).
27. L. Rogobete, F. Kaminski, M. Agio, and V. Sandoghdar, "Design of plasmonic nanoantennae for enhancing spontaneous emission," Opt. Lett. **32**, 1623–1625 (2007).
28. C. X. Cong, T. Yu, Z. H. Ni, L. Liu, Z. X. Shen, and W. Huang, "Fabrication of graphene nanodisk arrays using nanosphere lithography," JPCC **113**, 6529–6532 (2009).
29. R. Filter, J. Qi, C. Rockstuhl, and F. Lederer, "Circular optical nanoantennas: an analytical theory," Phys. Rev. B **85**, 125429 (2012).
30. C. A. Balanis, *Antenna Theory: Analysis and Design*, 3rd ed. (J. Wiley, New York, 2005).
31. R. Esteban, M. Laroche, and J.-J. Greffet, "Influence of metallic nanoparticles on upconversion processes," J. Appl. Phys. **105**, 033107 (2009).
32. P. Bharadwaj, B. Deutsch, and L. Novotny, "Optical antennas," Adv. Opt. Photon. **1**, 438–483 (2009).
33. A. Tielens, *The Physics and Chemistry of the Interstellar Medium* (Cambridge Univ Pr, 2005).
34. S. R. Langhoff, "Theoretical infrared spectra for polycyclic aromatic hydrocarbon neutrals, cations, and anions," J. Phys. Chem. **100**, 2819–2841 (1996).
35. M. Steglich, C. Jäger, G. Rouillé, F. Huisken, H. Mutschke, and T. Henning, "Electronic spectroscopy of medium-sized polycyclic aromatic hydrocarbons: implications for the carriers of the 2175 Å uv bump," ApJ **712**, L16 (2010).
36. P. Würfel, S. Finkbeiner, and E. Daub, "Generalized planck's radiation law for luminescence via indirect transitions," Appl. Phys. A-Mater. Sci. Process. **60**, 67–70 (1995).
37. S. M. Barnett and R. Loudon, "Sum rule for modified spontaneous emission rates," Phys. Rev. Lett. **77**, 2444–2446 (1996).
38. K. Joulain, J. Mulet, F. Marquier, R. Carminati, and J. Greffet, "Surface electromagnetic waves thermally excited: Radiative heat transfer, coherence properties and casimir forces revisited in the near field," Surf. Sci. Rep. **57**, 59–112 (2005).
39. A. Jones and M. Raschke, "Thermal infrared near-field spectroscopy," Nano Lett. **12**, 1475–1481 (2012).
40. A. L. Mattioda, A. Ricca, J. Tucker, C. W. Bauschlicher, and L. J. Allamandola, "Far-infrared spectroscopy of neutral coronene, ovalene, and dicoronylene," AJ **137**, 4054 (2009).
41. C. Rockstuhl and W. Zhang, "Terahertz optics: terahertz phase modulator," Nat. Photonics **3**, 130–131 (2009).
42. A. Vakil and N. Engheta, "Transformation optics using graphene," Science **332**, 1291–1294 (2011).
43. A. S. Mayorov, R. V. Gorbachev, S. V. Morozov, L. Britnell, R. Jalil, L. A. Ponomarenko, P. Blake, K. S. Novoselov, K. Watanabe, T. Taniguchi, and A. K. Geim, "Micrometer-scale ballistic transport in encapsulated

#180026 - $15.00 USD Received 16 Nov 2012; revised 21 Jan 2013; accepted 23 Jan 2013; published 6 Feb 2013

graphene at room temperature," Nano Lett. **11**, 2396–2399 (2011).
44. G. Y. Slepyan, S. A. Maksimenko, A. Lakhtakia, O. Yevtushenko, and A. V. Gusakov, "Electrodynamics of carbon nanotubes: Dynamic conductivity, impedance boundary conditions, and surface wave propagation," Phys. Rev. B **60**, 17136–17149 (1999).
45. V. P. Gusynin, S. G. Sharapov, and J. P. Carbotte, "Magneto-optical conductivity in graphene," J. Phys.: Condens. Matter **19**, 026222 (2007).
46. P.-Y. Chen and A. Alu, "Atomically thin surface cloak using graphene monolayers," ACS Nano **5**, 5855–5863 (2011).

1. Introduction

The advance of optical antennas has led to incredible new possibilities to control light-matter-interactions; including the directive emission of quantum systems or the modification of radiative rates at which such hybrid systems emit light. [1–3] The parameter usually used to quantify modified emission rates of quantum systems is the Purcell factor F defined as $F = \gamma_{\mathrm{rad}}^{\mathrm{a}}/\gamma_{\mathrm{rad}}^{\mathrm{fs}}$ with the radiative emission rate γ_{rad}. The superscripts "a" and "fs" denote the presence of the antenna or an emission in free space, respectively. For a cavity, F is proportional to the quality factor Q and λ^3/V, where λ is the wavelength and V is the mode volume. High Purcell factors have been achieved either in high-Q resonators, tolerating larger mode volumes, [4] or in systems supporting localized surface plasmon polaritons (LSPP) with extremely small mode volumes, therefore tolerating lower Q-factors [5–8]. However, since comparable Purcell factors appear for modes at higher frequencies in most of such implementations, these approaches are inappropriate for the selective enhancement of emissions at individual frequencies exclusively. Moreover, the impossibility to tune the spectral response of metal-based antennas over extended spectral domains is extremely restrictive for many applications. Mechanically tunable metallic cavities are however able to selectively enhance electric *or* magnetic dipole transitions [9].

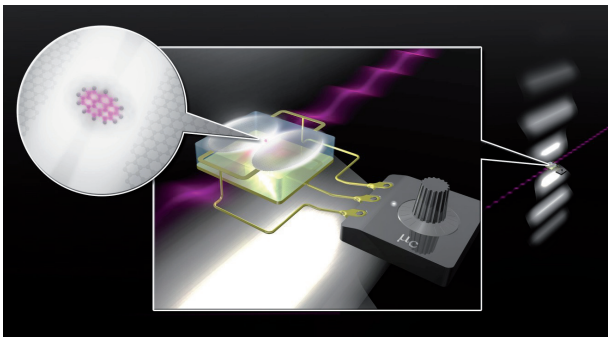

Fig. 1. A graphene antenna to selectively enhance THz emissions: A molecule gets excited in the visible/UV. Subsequentially, it strongly emits at a single frequency in the THz regime. The emission frequency can be tuned by adjusting the chemical potential μ_c.

Recently, graphene has been suggested as a possible material that may remedy at least some of these limitations [7]. Moreover, since its operational domain would be in the THz frequency range ($\nu \approx 0.1 - 30$ THz), it may also be used for long-needed functional devices in the so-called THz gap [10–12]. An example is the graphene antenna discussed in this work and visualized in Fig. 1. In the THz frequency domain, graphene offers low-loss SPPs [13–17], which have a lower loss than their metallic counterparts for two reasons, although graphene's advantage at this point is not extraordinary. First, the intrinsic losses are less since the electronic scattering rate is roughly one order of magnitude lower than Drude loss rates. Second, the one-atom

#180026 - $15.00 USD Received 16 Nov 2012; revised 21 Jan 2013; accepted 23 Jan 2013; published 6 Feb 2013

thick structure has a smaller cross section to the actual SPP mode. The effective wavelengths of propagating SPPs supported by graphene are two to three orders of magnitude smaller than the free space wavelengths at the same frequency [18]. The small wavelengths of the propagating SPP's on graphene are in turn implying small resonant structures supporting localized SPP's which are needed for high Purcell factors [19]. Most notably, the electronic properties of graphene can be widely tuned using the electric field effect [20–22]. A final advantage of graphene is that it does not support SPPs at optical frequencies [23]. This property is extremely useful for the selective enhancement of THz emission bands since optical emission bands are only marginally influenced by graphene antennas, i.e. one may assume $F_{\mathrm{rad}}\left(\omega_{\mathrm{optical}}\right) \approx 1$.

A referential example for an application in the THz domain is the identification of specific molecules, e.g., in any transmission, fluorescence, or Raman spectroscopy experiments which rely on previously collected spectroscopic information [24]. Although graphene-based optical antennas were already suggested to support such processes [7, 25], in principle, metal-based antennas can also be used in such applications. Therefore, the two key questions to be answered are: *How can graphene antennas be used to observe effects which are fundamentally inaccessible by metal antennas and how can basic limitations of the latter ones be overcome?*

Here we introduce a concept that allows the selective enhancement emissions in molecules using tunable THz antennas made of graphene. It will be shown that distinct and very weak spectral features at disparate frequencies can be enhanced without any structural modification of the antenna. The scheme we are going to introduce provides the possibility to probe for all spectral features of a certain molecule; thus simplifying the spectroscopic classification of the molecule tremendously. To enhance spectrally weak features, it is essential that the enhancement is selective, i.e. no other transitions shall be strongly enhanced except the desired one. This requires carefully designed antennas where higher-order resonances are shifted off the spectral domain of interest.

For this reason, we will discuss the optical properties of a graphene-based antenna and elaborate on the details of the ultimate design first. All spectral properties are clearly motivated by the requirements described above. We will also discuss the interaction of the antenna with a specific molecule and outline how its spectral properties can be selectively enhanced.

2. Efficient and tunable graphene antennas for strong spontaneous emission enhancement

As mentioned earlier, graphene SPPs are prone to losses. Therefore, the rate at which radiation can escape an antenna-emitter system γ_{rad} is lower than the total emission rate γ_{tot} of the emitter, $\gamma_{\mathrm{tot}} = \gamma_{\mathrm{loss}} + \gamma_{\mathrm{rad}}$. Both quantities are related by the antenna efficiency $\eta = \gamma_{\mathrm{rad}}/\gamma_{\mathrm{tot}}$. The enhancement F_{tot} of the total emission rate γ_{tot} of a dipole emitter in the vicinity of an antenna compared to the case of free space can be calculated within the Weisskopf-Wigner approximation as $F_{\mathrm{tot}} = \gamma^{\mathrm{a}}_{\mathrm{tot}}/\gamma^{\mathrm{fs}}_{\mathrm{tot}} = P^{\mathrm{a}}_{\mathrm{tot}}/P^{\mathrm{fs}}_{\mathrm{tot}}$ [26]. Here, $P^{\mathrm{a/fs}}_{\mathrm{tot}}$ is the total power emitted by the dipole. Using the latter relation, it is possible to calculate the emission rates in the realm of classical electrodynamics. Assuming that the emission in free space is free of absorption ($\eta^{\mathrm{fs}} = 1$), the Purcell factor with respect to the antenna reads as $F = \eta^{\mathrm{a}} F_{\mathrm{tot}}$. In general, F_{tot} depends on the position of the dipole, its polarization, and all properties of the antenna.

In the following, we will show how to achieve a high Purcell factor for a graphene-based antenna in the THz regime at a preselected frequency exclusively. The electric field effect can be used to change Graphene's chemical potential μ_c and consequentially its conductivity. See App. A for more information and details on our numerical implementation of the material. We further assume that the devices required to apply the electric field effect do not strongly influence the overall emission properties. This simplifies the analysis to free standing elements.

The design of plasmonic antennas with high efficiency η^a at a certain frequency strongly

#180026 - $15.00 USD Received 16 Nov 2012; revised 21 Jan 2013; accepted 23 Jan 2013; published 6 Feb 2013

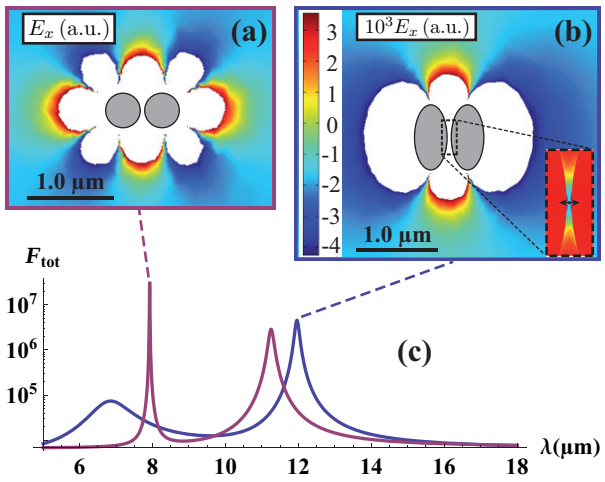

Fig. 2. (a) & (c) Two circular graphene elements cause a strong enhancement of the total emission rate F_{tot} for a dark antenna mode at $\lambda \approx 7.9\ \mu$m ($\nu \approx 38$ THz). To visualize the field outside the antenna, the colormap has been truncated (white regions). (b) & (c) The antenna with two elliptical elements exhibits by far the strongest F_{tot} for the desired dipolar mode at $\lambda \approx 12\ \mu$m ($\nu \approx 26.6$ THz). The scale shown in (b) applies for all field plots with order-of magnitude rescalings.

depends on geometrical parameters. Notably, the efficiency of sub-wavelength antennas can be quite low. To achieve a high Purcell factor, one thus encounters a trade-off between high F_{tot} and η^a. Plasmonic antennas consisting of two elements generally exhibit a larger efficiency than single element antennas [27]. In consequence, a configuration is considered where the dipole is situated in the center between the two elements of the antenna. The dipole is oriented in x-direction, i.e. parallel to the connection line of both elements. As a result of the strong confinement of the LSPP, a small separation between the antenna elements is required. Initially we chose an antenna design consisting of two circular elements. Such a device can be fabricated e.g. using nanosphere lithography and the single discs may be described as Fabry-Perot resonators [28, 29]. A configuration with radii of 200 nm and separation of 30 nm was found to exhibit $F_{\text{tot}} \approx 10^{6\ldots7}$, and an efficiency $\eta \approx 0.32$ at $\nu \approx 26.6$ THz with $\mu_c = 1$ eV. However, this structure also permits the coupling of the dipole to higher-order resonances of the antenna, see Fig. 2(a). These higher-order resonances, sometimes called dark modes, have extremely low efficiencies since they are only weakly coupled to the far-field. Nevertheless, they exhibit a strong F_{tot} and are therefore undesired. For our present scenario, a dark mode at $\nu \approx 38$ THz had an enhancement exceeding that of the dipole resonance with an efficiency of only $\eta \approx 0.035$. Therefore, these higher-order resonances have to be suppressed in order to render the device useful.

We found that the problem can be circumvented by stretching the discs in the vertical (y) direction, i.e. perpendicular to the dipole, by a factor of two. This stretching results in an increase of the effective radiating area of the antenna and thus of its efficiency. This is accompanied by a blueshift of the undesired higher-order modes [27]. We observed a suppression of these dark modes by several orders of magnitude for an antenna made of two elliptical elements. Another aspect in favor of our design is a further enhancement of F_{tot}, see Fig. 2(c). Generally, F_{tot} at other frequencies than the antenna's dipole resonance is two or more orders of magnitude smaller. This offset permits the desired selective enhancement of molecular resonances if the resonance of the antenna coincides with one of the resonances of a quantum system as it will

#180026 - $15.00 USD Received 16 Nov 2012; revised 21 Jan 2013; accepted 23 Jan 2013; published 6 Feb 2013

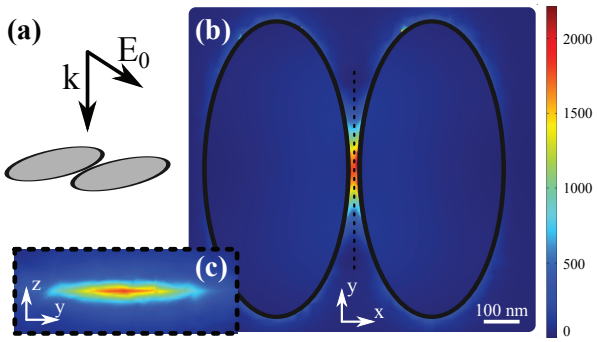

Fig. 3. (a) A plane wave with amplitude E_0 excites the dipolar resonance $\lambda \approx 12\,\mu$m of the antenna. (b) & (c): Distribution of $|\mathbf{E}(\mathbf{r})/E_0|$ in the plane of the graphene ellipses (x-y-plane) and in-between at $x = 0$ (y-z-plane). The region with strong enhancement is approximately $30 \times 100 \times 20\,\text{nm}^3$ (blue region). For a dipole situated here, the Purcell effect is comparable to a placement in the center.

be outlined in the following section.

One may furthermore ask the question how strongly localized the Purcell enhancement is for the found efficient antenna. Because of the plasmonic nature of the mode, one expects a rather small region of enhancement. To measure the size of this region, one can use the reciprocity theorem: [30–32] Illuminating the antenna with a plane wave corresponds to an emitting dipole at infinity. We assume that the plane wave excitation comes from a direction of strong emission of the antenna's dipole mode. Then, the field enhancement at some position is a measure for the radiated power of a dipole at that very position. We further assume that the dipole emitter couple to the dipole mode of the antenna. Then, radiation patterns do not change strongly for different emitter positions. Consequentially, the ratios of field enhancements are proportional to the ratios of the overall radiated power and thus the ratio of Purcell enhancements. We have made a corresponding calculation. As expected, we found a region of strong interaction confined in-between the antenna, see Fig. 3.

3. The changed spectrum of coronene

Up to this point, the enhancement of the total emission rate F_{tot} was referring to a dipole in the vicinity of a graphene antenna. To demonstrate the performance of the suggested implementation, coronene ($C_{24}H_{12}$) has been chosen as an example. It belongs to the group of polycyclic aromatic hydrocarbon (PAH) complexes and is of both great practical and theoretical interest [33]. The molecule exhibits resonances in the THz regime and its properties are well-documented [34, 35].

The emission process of coronene can be understood as a stepwise procedure following Ref. [33]. First, upon absorption of a UV photon, the electronic configuration of the molecule is transferred into an excited state. The excitation will be assumed in the near ultraviolet around a frequency of $\sim 990\,\text{THz}$ (300 nm) where coronene absorbs strongly. The absorbed energy is then almost instantaneously redistributed to the different vibrational modes of the molecule. The characteristic time scale of this process is about $10^{-12}\,\text{s}$. This redistribution obeys a Planck distribution $B(\omega; T_{\text{m}})$ over the respective eigenenergies $\hbar\omega_i$. The temperature T_{m} refers to the microcanonical temperature of the molecule and can be approximated by $T_{\text{m}} \simeq 2000\,(E\,(eV)/N_{\text{c}})^{0.4}\,K$ with the energy of the exciting radiation E in electronvolts and the number $N_{\text{c}} = 24$ of carbon atoms of coronene. The expression for T_{m} can be derived

#180026 - $15.00 USD Received 16 Nov 2012; revised 21 Jan 2013; accepted 23 Jan 2013; published 6 Feb 2013

from the density of states of PAH's. It has been proven correct within an error of $\approx 10\%$ for $35\ldots1000\,\mathrm{K}$ [33]. For coronene and the given excitation, we get $T_\mathrm{m} \approx 990\,\mathrm{K}$. The emission spectrum in free space is then given by the oscillator strengths $f(\omega_i)$ weighted by $B(\omega;T_m)$ [33]. This behaviour corresponds to the generalized Planck radiation law for luminescence and holds for a large class of molecules, semiconductors etc.; see e.g. Ref. [36].

Close to the antenna, the emission of the molecule is strongly modified. We assume here, that the redistribution of energy into the different eigenmodes is much faster than any involved radiation process. This seems reasonable since the natural emission time for THz radiation is in the order of or even bigger than one second [33]. Therefore, one might hypothesize that even an enhancement of several orders of magnitude for the given THz transitions in coronene should be possible without any noticeable influence on the internal redistribution dynamics. Hence, by enhancing the emission rate for just one eigenmode, the emission of the remaining ones decreases. Then, one finds different total emission rate enhancements for each transition $\mathscr{F}_\mathrm{tot}(\omega_i)$, which deviate from the Purcell factors of a single dipole, i.e. $\mathscr{F}_\mathrm{tot}(\omega_i) \neq F_\mathrm{tot}(\omega_i)$. For a linear multiresonant system, modified emission rates are related to each other by a sum rule [37]. Because of the internal redistribution dynamics of coronene, this approach cannot be used. We assume that the power emitted upon excitation does not change if the antenna is present, i.e., $P^\mathrm{a}_\mathrm{tot} = \sum_i \hbar\omega_i\gamma_i\mathscr{F}(\omega_i)B(\omega_k;T_\mathrm{m}) \stackrel{!}{=} P^\mathrm{fs}_\mathrm{tot}$ implying energy conservation. Then, the enhancement of the radiative rate with respect to the antenna efficiency is given by

$$\begin{aligned}\mathscr{F}_\mathrm{rad}(\omega_i) &= \eta(\omega_i)\cdot F_\mathrm{tot}(\omega_i)\cdot \\ &\qquad \frac{\sum_k \hbar\omega_k\gamma^\mathrm{fs}_\mathrm{tot}(\omega_k)B(\omega_k;T_\mathrm{m})}{\sum_k \hbar\omega_k F_\mathrm{tot}(\omega_k)\gamma^\mathrm{fs}_\mathrm{tot}(\omega_k)B(\omega_k;T_\mathrm{m})}\,. \end{aligned} \tag{1}$$

Since the characteristics of the graphene antenna can be tuned by changing the chemical potential μ_c, the enhancement also depends on μ_c. If now a certain transition is selectively enhanced to a large extent, $F_\mathrm{tot}(\omega_i) \gg F_\mathrm{tot}(\omega_k)\ (k\neq i)$, the energy supplied to the molecule will predominantly leave it by exactly this transition. This result would also hold with respect to the sum rule in Ref. [37], for which we would find $\mathscr{F}^\mathrm{BSL}_\mathrm{tot}(\omega_i) = F_\mathrm{tot}(\omega_i)/\sum_k F_\mathrm{tot}(\omega_k)$. Hence, it might be expected that the shift of emission processes in favor of a single transition by a selective enhancement is likely to be a generic property of molecular systems.

A temperature T of the environment also changes the emission rates of molecules [38, 39]. Then the condition for selective enhancement changes to $F_\mathrm{tot}(\omega_i)\cdot B(\omega_i;T) \gg F_\mathrm{tot}(\omega_k)B(\omega_k;T)\ (k\neq i)$. Hence, the selective enhancement is working for all frequencies ω_i if the difference in F_tot is much more significant than the differences of temperature induced emissions, which is generally the case for a coupling to resonant systems [38].

The spectral resolution of the selective enhancement is limited by the antenna. It is naturally linked to the width of the antenna resonance which is approximately the relaxation rate Γ. So, if Γ is smaller than the minimum spectral distance between certain resonances one wishes to distinguish, the selective enhancement should work. This is the case for coronene; current fabrication techniques allow relaxation rates in the order of a few meV or THz, respectively [21].

To demonstrate this selective *and* tunable enhancement, Fig. 4 shows how the emission spectrum of coronene changes if the antenna resonances are tuned. Although extensive simulations were performed, only a few selective results are shown where the resonance was tuned to enhance the emission at frequencies corresponding to "jumping-jack"-, "drumhead"- and a "C-H-out-of-plane"-vibrational motion at 11.3 THz, 16.5 THz and 26.0 THz, respectively [40]. Noteworthy, these emissions are electric dipole-allowed, consistent with our analysis of the graphene antenna. The quantitative visualization of the spectra is performed by assuming, as usual, a certain line width for each resonance. For PAH's, we used a linewidth of $0.15\,\mathrm{THz}$,

#180026 - $15.00 USD Received 16 Nov 2012; revised 21 Jan 2013; accepted 23 Jan 2013; published 6 Feb 2013

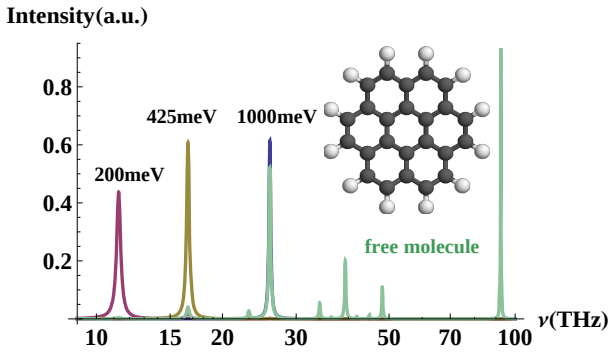

Fig. 4. The modified emission spectrum of coronene in the vicinity of the graphene antenna as a function of the chemical potential μ_c. For reference, the green curve displays the emission spectrum of the bare molecule exhibiting several peaks with different strengths. When tuning the chemical potential by taking advantage of the electric field effect, the antenna may strongly *and* selectively enhance only a single emission line, so that most of the energy leaves the molecule via this transition.

which is characteristic for molecules isolated from each other [40]. It can be clearly seen that by tuning the antenna it is possible to choose the transition which is forced to emit light into the far-field; the main goal of this contribution. Various effects might broaden the lines as e.g. the coupling to surfaces or collisions with other molecules. Nevertheless, it can be safely anticipated that the general characteristics of the spectrum survive.

4. Conclusion

In conclusion, we have suggested and verified that due to the unique properties of graphene, antennas made from this material can be used to selectively enhance different molecular transitions at THz frequencies by several orders of magnitude. The achievable efficiencies and the suppression of undesired modes were found to strongly depend on the actual antenna geometry. A suitable implementation which consists of two closely placed elliptical graphene elements was introduced. Using this antenna, weak transitions can be made dominant in the emission spectrum. The potential of graphene antennas to selectively enhance molecular transitions can clearly be anticipated to lead to new applications in THz spectroscopy but will also contribute to the development of novel sensors, highly directed single photon light sources, and quantum communication and quantum computation devices [41].

A. Numerical implementation of graphene

At temperature T, the in-plane conductivity of graphene can be approximated using the Kubo formula

$$\begin{aligned}\sigma_s(\omega) &= \mathrm{i}\frac{1}{\pi\hbar^2}\frac{e^2 k_B T}{\omega+\mathrm{i}2\Gamma}\left\{\frac{\mu_c}{k_B T}+2\ln\left[\exp\left(-\frac{\mu_c}{k_B T}\right)+1\right]\right\} \\ &\quad +\mathrm{i}\frac{e^2}{4\pi\hbar}\ln\left[\frac{2|\mu_c|-\hbar(\omega+\mathrm{i}2\Gamma)}{2|\mu_c|+\hbar(\omega+\mathrm{i}2\Gamma)}\right] \end{aligned} \quad (2)$$

with the chemical potential μ_c and the relaxation rate Γ [7, 18]. Γ was taken to be 0.1 meV, consistent with values reported earlier [42]. Γ may also be calculated from experimental data for the transport mobility [43]. Note that the second interband term is not temperature dependent

#180026 - $15.00 USD Received 16 Nov 2012; revised 21 Jan 2013; accepted 23 Jan 2013; published 6 Feb 2013

for $k_B T \ll |\mu_c|$. This is in very good approximation for the values of the chemical potential used in our analysis, even at room temperature, where $k_B T \approx 26\,\mathrm{meV}$. Throughout, we assumed a time dependency according to $\exp(-\mathrm{i}\omega t)$. In our calculations, we represented graphene as a thin conductive layer with thickness $d = 1\,\mathrm{nm} \ll \lambda$ and relative permittivity $\varepsilon_g(\omega) = 1 + \mathrm{i}\sigma_s(\omega)/(\varepsilon_0\,\omega\,d)$, see also Refs. [7, 18, 44–46] and [42]. It was verified that none of the results are quantitatively affected by that finite thickness. All simulations were performed using the Finite-Element Method as implemented in COMSOL Multiphysics 3.5. It may be explicitly noted that we take any non-radiative loss into account via the losses in the graphene antenna and through the internal redistributions in coronene.

Acknowledgments

We thank Karsten Verch (www.karstenverch.com) for his artistic view of the theory in Fig. 1. We also appreciate the professional feedback and further input of the anonymous reviewers to state certain points more clearly. Financial support by the German Federal Ministry of Education and Research (PhoNa), by the Thuringian State Government (MeMa) and the German Science Foundation (SPP 1391 Ultrafast Nano-optics) is acknowledged.

#180026 - $15.00 USD Received 16 Nov 2012; revised 21 Jan 2013; accepted 23 Jan 2013; published 6 Feb 2013